Since January 2020 Elsevier has created a COVID-19 resource centre with free information in English and Mandarin on the novel coronavirus COVID-19. The COVID-19 resource centre is hosted on Elsevier Connect, the company's public news and information website.

Scientific African 12 (2021) e00811

Contents lists available at ScienceDirect

Scientific African

journal homepage: www.elsevier.com/locate/sciaf

Mathematical assessment of the role of denial on COVID-19 transmission with non-linear incidence and treatment functions

Reuben Iortyer Gweryina*, Chinwendu Emilian Madubueze, Francis Shienbee Kaduna

Department of Mathematics/Statistics/Computer Science, University of Agriculture, P.M.B. 2373, Makurdi, Nigeria

ARTICLE INFO

Article history:
Received 21 January 2021
Revised 29 May 2021
Accepted 4 June 2021

Editor: DR B. Gyampoh

Keywords:
COVID-19
Denial
Non-linear incidence
Backward bifurcation
Global stability
Optimal control analysis

ABSTRACT

A mathematical model describing the dynamics of Corona virus disease 2019 (COVID-19) is constructed and studied. The model assessed the role of denial on the spread of the pandemic in the world. Dynamic stability analyzes show that the equilibria, disease-free equilibrium (DFE) and endemic equilibrium point (EEP) of the model are globally asymptotically stable for $R_0 < 1$ and $R_0 > 1$, respectively. Again, the model is shown via numerical simulations to possess the backward bifurcation, where a stable DFE co-exists with one or more stable endemic equilibria when the control reproduction number, R_0 is less than unity and the rate of denial of COVID-19 is above its upper bound. We then apply the optimal control strategy for controlling the spread of the disease using the controllable variables such as COVID-19 prevention, hospitalization and maximum treatment efforts. Using the Pontryagin maximum principle, we derive analytically the optimal controls of the model. The aforementioned control strategies are performed numerically in the presence of denial and without denial rate. Among such experiments, results without denial have shown to be more productive in ending the pandemic than others where the denial of the disease invalidates the effectiveness of the controls causing the disease to continue ravaging the globe.

1. Introduction

Coronavirus disease 2019 (COVID-19) is a respiratory disease of the Coronavidae family. The virus has four types of strains, namely; α-Coronavirus, β-Coronavirus, γ-Coronavirus and δ-Coronavirus. The first two affects humans and the last two are known majorly for birds infection [1]. The origin and the reservoir of the virus still remain uncertain, even though Singh et al. [2] considers COVID-19 to be zoonotic disease and traced it to the bats family. COVID-19 is the 3rd novel coronavirus in the 21st century after SARS and MERS to have caused large epidemic that spread over 210 nations worldwide [3].

* Corresponding author.
E-mail addresses: gweryina.reuben@uam.edu.ng (R.I. Gweryina), ce.madubueze@gmail.com (C.E. Madubueze), kadunafrancis@gmail.com (F.S. Kaduna).

https://doi.org/10.1016/j.sciaf.2021.e00811

COVID-19 is a pandemic of all ages when compare to SARS and MERS. It can spread rapidly among the elderly and individuals with underlying medical conditions, who are particularly a severe risk population [4]. Human-to-human transmission can occur when the respiratory droplets of an asymptomatic, pre-symptomatic and symptomatic person touches the nose, eyes or mouth of a susceptible individual on a closed contact [5]. The clinical symptoms of the disease such as cough, breathing difficulty, fever among other malarial related signs begin to manifest within 5–6 days on average during the incubation period of the virus [6].

The cure for this disease is still a problem facing nations, and the hope for guaranteed vaccine formulation though not a lost one but yet to be made available. As a result, an index case that began in Wuhan, China has spread to many countries and is responsible for over 1 940 529 deaths globally, 72 834 deaths in Africa [7] and 1405 deaths in Nigeria [8] as of January 14, 2021.

In addition, the above number of human deaths in Nigeria is due to the lack of willingness of the populace to accept the existence of COVID-19 [9]. Some are of the opinion that COVID-19 cases in Nigeria have been mutilated for political gains. Based on such psychological thoughts, many vulnerable populations have lost confidence in getting protective measures as recommended by World Health Organization (WHO) [4] and Nigeria Center for Disease Control(NCDC) [8]. From the past epidemics, transmission indices have shown that the denial of existence of a disease indeed stands a challenge for epidemiologists in the fight against the disease prevention and control. See for example, the denial effect of HIV/AIDS [10,11] on susceptible population. Apart from denial, people who use both licit and illicit drugs pause a greater problem in harm reduction interventions in the era of COVID-19 in Africa [12].

Non-linear incidence and treatment functions have been reported by several authors [13–15] to be invaluable tool used to reduce the spread of diseases, not limited to measles and tuberculosis. In epidemiological modelling of COVID-19, mass action function of the kind βSI, where β is the infection rate was applied in model of [16] and a saturated incidence rate, $\frac{\alpha SI}{1+\beta S}$ was found in the models of [17,18]. On the other hand, the application of Beddington-De Angelis incidence rate of type $\frac{\alpha SI}{1+\beta S+\gamma I}$ was adopted in the works of [19–23] for non-COVID-19 models.

Treatment has been the integral part of the solution of epidemic outbreak considered at different rates. So far, Adeniyi et al. [24] and Daniel [18] used a constant rate and Holling type II, $\frac{\beta I}{1+\gamma I}$ respectively as treatment functions, in corona virus transmission models. Other controls such as lock down strategy, social isolation on corona virus have been deliberated upon in the work of Ndam [16] without denial effect. A dual-purpose wheelchair was developed for containment of COVID-19 in paraplegic patients in Lagos, Nigeria [25], and knowledge and attitudinal behaviour among Sudanese population was also observed to be key in eradicating the pandemic [26].

In this paper, we intend to assess the role of denial on the optimal control model for COVID-19 transmission dynamics using Beddington-De Angelis incidence and treatment function of Holling type II. To the best knowledge of the authors, this has not been applied on any mathematical model as regards to COVID-19 pandemic. Our model made advances to existing works on COVID-19 in the following dimensions:

(i) we incorporate denial as an erroneous human behaviour that triggers the spread of COVID-19 among Africans. In mathematical sense, the consideration of this invaluable factor is a novelty.
(ii) The introduction of denial on Beddegton-De Angelis function is unique compared to other existing mathematical models on COVID-19.
(iii) The inclusion of a non-linear maximal treatment function as a pharmaceutical strategy in the control of COVID-19 is also a new idea compared to other models in literature.

This paper is organized as follows: we introduce the model formulation in Section 2. Equilibria analysis of the proposed model is given in Sections 3 and 4. An optimal control analysis is done in Section 5. Meanwhile numerical results and discussion are given in Section 6. Section 7 describes the conclusion of the paper.

2. Materials and methods

2.1. Model formulation

In this study, we propose a mathematical framework of generic SEIR model for COVID-19 transmission dynamics using the Beddington-De Angelis functional response and Holling type II treatment as applied in [15,16] on infectious model. The derivation of the differential equations is as a result of the under listed assumptions:

a. The total population, N at any time, t, is divided into five classes: Susceptible people, S (who are under risk of contracting COVID-19), Exposed people, E (who are in close contact with infected people, but not yet infected), Asymptomatic people, A (who harbour the corona virus without clinical symptoms but capable of transmitting the disease), Symptomatic people, I (who are infected with the corona virus with clinical symptoms and capable of transmitting the disease), Hospitalized people, H (infectious people who are isolated for treatment) and Recovered people, R (who survived the COVID-19 infection). Thus, $N = S + E + A + I + H + R$.
b. The susceptible people are recruited at the constant rate, $\hat{B}$ and die naturally like others at a rate μ.

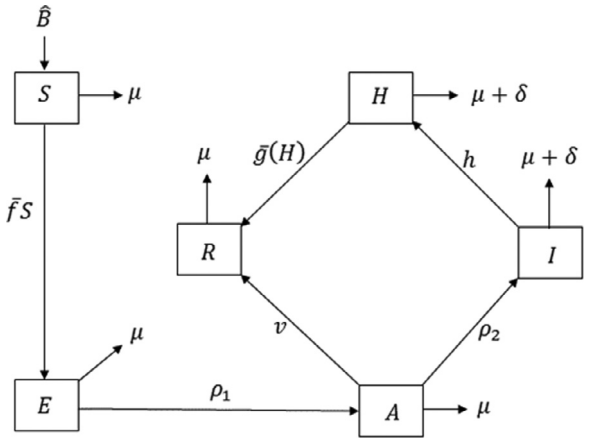

Fig. 1. Schematic diagram for COVID-19 transmission dynamics.

c. COVID-19 is transmitted from Asymptomatic people, Symptomatic people, Hospitalized/isolated people to susceptible people by Beddington-De Angelis incidence rate in Eq. 1,

$$\hat{f} = \frac{\beta S(c_1 A + c_2 I + c_3 H)}{1 + (\eta_1 - d)(S + E + A) + \eta_2 I + \eta_3 H}, \tag{1}$$

where β is the average infection rate, $c_i, i = 1, 2, 3$ $(c_1 > c_2 > c_3)$ is the contact rate of susceptible with A, I and H respectively, d is the denial effect rate, η_1 refers to the measure of inhibition effect of preventive protocols such as social distancing, use of face masks and hand sanitizers taken by both susceptible and exposed people. Meanwhile, η_2, η_3 are measures of inhibition effect due to maximum treatment with respect to infectious people, I and H respectively. Note that $0 < \eta_1 - d < \eta_2 < \eta_3$ when denial of the disease exist. It is of great interest to reveal that, four kinds of incidence rates can be obtainable from this Beddington-De Angelis incidence, (i. e; Eq. 1) in this proposed study:

i. if we set $\eta_1 = d, \eta_2 = \eta_3 = 0$, then $\bar{f}(S, A, I, H) = \beta S(c_1 A + c_2 I + c_3 H)$, which is bilinear incidence rate (force of mass action).
ii. if we set $\eta_2 = \eta_3 = c_2 = c_3 = 0$, then $\bar{f}(S, E, A) = \frac{\beta S c_1 A}{1+(\eta_1 - d)(S+E+A)}$, which is saturation incidence rate with the sum of susceptible and exposed people (infectious of COVID-19 without symptoms). This inhibition effect is as a result of saturation parameter η_1 which is the preventive protocol to control the spread of the pandemic.
iii. if we set $\eta_1 = d, \eta_3 = c_1 = c_3 = 0$, then $\bar{f}(S, I) = \frac{\beta S c_2 I}{1+\eta_2 I}$, which is saturation incidence rate with infectious people (yet to be isolated/hospitalized). Here, the contact between susceptible and infectious people, may saturate at high transmission level due to crowding of infectious people or protection from the susceptible people.
iv. if we set $\eta_1 = d, \eta_2 = c_1 = c_2 = 0$, then $\bar{f}(S, H) = \frac{\beta S c_3 H}{1+\eta_3 H}$, which is saturation incidence rate with hospitalized/isolated people. As in case (iii), the contact between isolated and susceptible people, may saturate at high transmission level due to crowding of isolated people or protection taken by the susceptible people.

d. the hospitalized people recovered by saturated Holling type II treatment rate is given by Eq. 2,

$$\bar{g}(H) = \frac{\gamma H}{1 + \epsilon H}, \tag{2}$$

with γ being the maximum treatment and ϵ measures the inhibition recovered rate due to long time response of hospitalized people to treatment. Note that ϵ is a constant parameter that accounts for the limited resource available for the treatment of COVID-19. The Asymptomatic people may recover earlier at a rate, ν.

e. The recovered people gain permanent immunity since no case of COVID-19 re-infection has been reported.
f. COVID-19 is a fatal disease with a death rate, δ.
g. The exposed progress to Asymptomatic class at a rate, ρ_1 before further developing symptoms of the disease at a rate, ρ_2. This assumption is supported by the works of Alshammari [27] and Deressa and Duressa [28].
h. Asymptomatic individuals who are infected without symptoms also deny the existence of the disease.

The summary of model parameter values and description is given in Table 1 below.

2.2. The model

Using the flow-diagram of the interacting population in Fig. 1, we obtain the differential coefficient of the variables as indicated in system 3.

$$\begin{aligned}
\frac{dS}{dt} &= \hat{B} - \bar{f}S - \mu S,\\
\frac{dE}{dt} &= \bar{f}S - (\mu+\rho_1)E,\\
\frac{dA}{dt} &= \rho_1 E - (\mu+\nu+\rho_2)A,\\
\frac{dI}{dt} &= \rho_2 A - (\mu+\delta+h)I,\\
\frac{dH}{dt} &= hI - \bar{g}(H) - (\mu+\delta)H,\\
\frac{dR}{dt} &= \nu A + \bar{g}(H) - \mu R,
\end{aligned} \tag{3}$$

where $\bar{f}$ and $\bar{g}(H)$ are as in Eqs. 1 and 2, with initial conditions

$$S(0) = S_0 > 0; E(0) = E_0 \geq 0; A(0) = A_0 \geq 0; I(0) = I_0 \geq 0; H(0) = H_0 \geq 0; R(0) = R_0 \geq 0.$$

It is obvious from Eq. 1 that once the dynamics of (S, E, A, I, H) are understood, then the dynamics of R immediately follows from the Eq. 4

$$\frac{dR}{dt} = \nu A + \bar{g}(H) - \mu R. \tag{4}$$

Therefore, from onwards, our study shall be focused on the reduced system below

$$\begin{aligned}
\frac{dS}{dt} &= \hat{B} - \bar{f}S - \mu S\\
\frac{dE}{dt} &= \bar{f}S - (\mu+\rho_1)E\\
\frac{dA}{dt} &= \rho_1 E - (\mu+\nu+\rho_2)A\\
\frac{dI}{dt} &= \rho_2 A - (\mu+\delta+h)I\\
\frac{dH}{dt} &= hI - \bar{g}(H) - (\mu+\delta)H
\end{aligned} \tag{5}$$

whose positivity and boundedness of solution can be verify in the next subsection.

2.3. Existence and uniqueness of solution

The epidemiological validity of the mathematical model in Eq. 5 rely on the solution of the dynamic system being positive and bounded for all time $t > 0$. This is to be established in the following theorems.

Theorem 2.1. *(positivity) If $t > 0$ and the starting conditions $\Gamma(0) \geqslant 0$, where*

$$\Gamma(t) = (S(t) > 0, E(t) > 0, A(0) > 0, I(t) > 0, H(0) > 0),$$

then the solution of Eq. 5 is non-negative provided they exist.

Proof. With the method in Alshammari [27], let $t_1 = \{t > 0 : \Gamma(t) > 0 \in [0, t]\}$, then it follows from the first Eq. 5 that

$$\frac{dS}{dt} = \hat{B} - \left(\frac{\beta S(t)(c_1A(t) + c_2I(t) + c_3H(t))}{1 + (\eta_1 - d)(S(t) + E(t) + A(t)) + \eta_2 I(t) + \eta_3 H(t)}\right)S(t) - \mu S(t) \tag{6}$$

Eq. 6 can be re-arranged as

$$\frac{dS}{dt}\left\{S(t)exp\left(\mu t + \beta\int_0^t \left(\frac{(c_1A(\tau) + c_2I(\tau) + c_3H(\tau))}{1 + (\eta_1 - d)(S(t) + E(t) + A(t)) + \eta_2 I(t) + \eta_3 H(\tau)}\right)S(\tau)d\tau\right)\right\}$$

$$-\hat{B}exp\left(\mu t + \beta\int_0^t \left(\frac{(c_1A(\tau) + c_2I(\tau) + c_3H(\tau))}{1 + (\eta_1 - d)(S(t) + E(t) + A(t)) + \eta_2 I(t) + \eta_3 H(\tau)}\right)S(\tau)d\tau\right) = 0$$

Thus,

$$S(t_1)exp\left(\mu t_1 + \beta\int_0^{t_1} \left(\frac{(c_1A(\tau) + c_2I(\tau) + c_3H(\tau))}{1 + (\eta_1 - d)(S(t) + E(t) + A(t)) + \eta_2 I(t) + \eta_3 H(\tau)}\right)S(\tau)d\tau\right) - S(0)$$

$$= \int_0^{t_1} \hat{B}exp\left(\mu\lambda + \beta\int_0^{\lambda} \left(\frac{(c_1A(\tau) + c_2I(\tau) + c_3H(\tau))}{1 + (\eta_1 - d)(S(t) + E(t) + A(t)) + \eta_2 I(t) + \eta_3 H(\tau)}\right)S(\tau)d\tau\right)d\lambda$$

from which we get

$$S(t_1) = S(0)exp\left\{-\left(\mu t_1 + \beta\int_0^{t_1} \left(\frac{(c_1A(\tau) + c_2I(\tau) + c_3H(\tau))}{1 + (\eta_1 - d)(S(t) + E(t) + A(t)) + \eta_2 I(t) + \eta_3 H(\tau)}\right)S(\tau)d\tau\right)\right\}$$

$$+exp\left\{-\left(\mu t_1 + \beta\int_0^{t_1} \left(\frac{(c_1A(\tau) + c_2I(\tau) + c_3H(\tau))}{1 + (\eta_1 - d)(S(t) + E(t) + A(t)) + \eta_2 I(t) + \eta_3 H(\tau)}\right)S(\tau)d\tau\right)\right\}$$

$$\times \int_0^{t_1} \hat{B} exp\Big(\mu\lambda + \beta \int_0^{\lambda} \Big(\frac{(c_1A(\tau) + c_2I(\tau) + c_3H(\tau))}{1 + (\eta_1 - d)(S(t) + E(t) + A(t)) + \eta_2 I(t) + \eta_3 H(\tau)}\Big) S(\tau) d\tau\Big) d\lambda > 0.$$

Therefore, $S(t)$ is non-negative for $t > 0$. In a similar fashion, it can be proven that $E > 0, A > 0, I > 0$ and $H > 0$ for $t > 0$. □

Theorem 2.2 (*boundedness*)**.**

$$\hat{\psi} = \Big\{(S(t), E(t), A(t), I(t), H(t)) \in R_+^5 \cup \{0\} : 0 < S(t) + E(t) + A(t) + I(t) + H(t) \leq \frac{\hat{B}}{\mu}\Big\}$$

is the positive feasible region of Eq. 5 containing non-negative starting conditions in R_+^5

Proof. Assume $N_1 = S(t) + E(t) + A(t) + I(t) + H(t)$ holds for $t > 0$, then we obtain

$$\frac{dS}{dt} = \hat{B} - \mu N_1(t) - \delta(I(t) + H(t)) - \frac{\gamma H(t)}{1 + \epsilon H(t)} \leqslant \hat{B} - \mu N_1(t) \tag{7}$$

By integrating Eq. 7, we get

$$N_1(t) \leqslant \frac{\hat{B}}{\mu} + (N_1(0) - \frac{\hat{B}}{\mu}) \exp(-\mu t) \tag{8}$$

Therefore $\lim_{t\to\infty} \sup N_1(t) \leqslant \frac{\hat{B}}{\mu}$. In addition, $\frac{dN_t}{dt} < 0$ if $N_1(0) > \frac{\hat{B}}{\mu}$. This indicates that all solutions of the model 5 remain in ψ, which is uniformly bounded and well-behaved. □

Theorem 2.3 (*uniqueness*)**.** *For the Model system 5 if the starting values* $S(0) > 0, E(0) > 0, A(0) > 0, I(0) > 0, H(0) > 0$ *and* $t_0 > 0$*, then for all* $t > 0$ *the solutions* $S(t), E(t), A(t), I(t)$ *and* $H(t)$ *exist and is unique in* R_+^5.

Proof. Based on the methodology in Deressa and Duressa [28], we rewrite the model system 5 in the form $x' = g(x)$,where

$$x' = \Big(S(t), E(t), A(t), I(t), H(t)\Big)^T,$$

$$g(x) = \begin{pmatrix} \hat{B} - (\frac{\beta(c_1A + c_2I + c_3H)}{1+(\eta_1-d)(S+E+A)+\eta_2 I+\eta_3 H})S - \mu S \\ (\frac{\beta(c_1A + c_2I + c_3H)}{1+(\eta_1-d)(S+E+A)+\eta_2 I+\eta_3 H})S - (\mu + \rho_1)E \\ \rho_1 E - (\mu + \nu + \rho_2)A \\ \rho_2 A - (\mu + \delta + h)I \\ hI - \frac{\gamma H}{1+\epsilon H} - (\mu + \delta)H \end{pmatrix}$$

For a singular reason, that g has a continuous first derivative in R_+^5, it is locally Lipschitz. With the fundamental theorem on existence and uniqueness of solution [30] and Theorems 2.1 and 2.2 established above, we can conclude that the Model system 5 has a solution that is unique, positive and bounded in R_+^5. □

3. Equilibria analysis

3.1. The disease-free equilibrium and the basic reproduction number

At the steady state, the disease-free equilibrium $D_0(S_0, E_0, A_0, I_0, H_0)$ of the System 5 was found at the point COVID-19 does not persist, and is given by $D_0 = (\frac{\hat{B}}{\mu}, 0, 0, 0, 0)$. Basic reproduction number which is computed at DFE is the strength of stability analysis of an epidemiological model. It is an essential threshold that predicts whether the spread of an infection continues or discontinues in a population. For our study, basic reproduction number is the average number of COVID-19 secondary cases generated by an index case when introduced in wholly COVID-19 virgin population. It is traditionally denoted by, R_0. For Model 5, we compute R_0 with the use of the next generation matrix method [31], focusing only on A, I, H being the infected compartments. Based on the principle of this method, the infection matrix, F and the transition matrix, V, evaluated at *DFE* are given respectively in Eq. 9

$$F = \begin{pmatrix} 0 & \frac{\beta S_0 c_1}{1+(\eta_1-d)S_0} & \frac{\beta S_0 c_2}{1+(\eta_1-d)S_0} & \frac{\beta S_0 c_3}{1+(\eta_1-d)S_0} \\ 0 & 0 & 0 & 0 \\ 0 & 0 & 0 & 0 \\ 0 & 0 & 0 & 0 \end{pmatrix} \quad \text{and} \quad V = \begin{pmatrix} \mu + \rho_1 & 0 & 0 & 0 \\ -\rho_1 & \mu + \nu + \rho_2 & 0 & 0 \\ 0 & -\rho_2 & \mu + \delta + h & 0 \\ 0 & 0 & -h & \mu + \delta + \gamma \end{pmatrix} \tag{9}$$

With that, R_0 which is expressed mathematically as the spectral radius of the next generation matrix, FV^{-1} is given by Eq. 10

$$\begin{aligned} R_0 &= \rho(FV^{-1}) \\ &= \frac{\beta S_0 c_1 \rho_1}{(\mu+\rho_1)(\mu+\nu+\rho_2)(1+(\eta_1-d)S_0)} + \frac{\beta S_0 c_2 \rho_1 \rho_2}{(\mu+\rho_1)(\mu+\nu+\rho_2)(\mu+\delta+h)(1+(\eta_1-d)S_0)} \\ &+ \frac{\beta S_0 c_3 \rho_1 \rho_2 h}{(\mu+\rho_1)(\mu+\nu+\rho_2)(\mu+\delta+h)(\mu+\delta+\gamma)(1+(\eta_1-d)S_0)} = R_{0A} + R_{0I} + R_{0H}, \end{aligned} \tag{10}$$

where the three components of R_0 in Eq. 10 measure the contribution of COVID-19 infection from asymptomatic to susceptible (R_{0A}), symptomatic to susceptible (R_{0I}) and hospitalized to susceptible (R_{0H}), respectively.

3.2. Local stability of disease-free equilibrium

Theorem 3.1. *The COVID-19 free equilibrium, $D_0 = (\frac{\hat{\beta}}{\mu}, 0, 0, 0)$ is locally asymptomatically stable if $R_0 < 1$ and unstable when $R_0 > 1$.*

Proof. The community matrix of the Model system (5) at disease-free state is given by Eq. 11.

$$J(D_0) = \begin{pmatrix} -\mu & 0 & -\frac{\beta S_0 c_1}{1+(\eta_1-d)S_0} & -\frac{\beta S_0 c_2}{1+(\eta_1-d)S_0} & -\frac{\beta S_0 c_3}{1+(\eta_1-d)S_0} \\ 0 & -\sigma_1 & \frac{\beta S_0 c_1}{1+(\eta_1-d)S_0} & \frac{\beta S_0 c_2}{1+(\eta_1-d)S_0} & \frac{\beta S_0 c_3}{1+(\eta_1-d)S_0} \\ 0 & \rho_1 & -\sigma_2 & 0 & 0 \\ 0 & 0 & \rho_2 & -\sigma_3 & 0 \\ 0 & 0 & 0 & h & -\sigma_4 \end{pmatrix}, \tag{11}$$

where

$\sigma_1 = \mu + \rho_1$, $\sigma_2 = \mu + \nu + \rho_2$, $\sigma_3 = \mu + \delta + h$, $\sigma_4 = \mu + \delta + \gamma$.

From the community matrix $J(D_0)$, we obtain the eigenvalue $\lambda = -\mu$ and Eq. 12

$$\lambda^4 + m_3\lambda^3 + m_2\lambda^2 + m_1\lambda + m_0 = 0, \tag{12}$$

where

$$\begin{aligned} m_3 &= \sigma_1 + \sigma_2 + \sigma_3 + \sigma_4, \\ m_2 &= \sigma_1\sigma_2(1 - R_{0A}) + (\sigma_1 + \sigma_2)(\sigma_3 + \sigma_4) + \sigma_3\sigma_4, \\ m_1 &= \sigma_1\sigma_2\sigma_3(1 - R_{0A} - R_{0I}) + \sigma_1\sigma_2\sigma_4(1 - R_{0A}) + \sigma_3\sigma_4(\sigma_1 + \sigma_2), \\ m_0 &= \sigma_1\sigma_2\sigma_3\sigma_4(1 - R_0), \end{aligned} \tag{13}$$

By Routh-Hurwitz criteria [32], Eq. 12 has negative real roots if the coefficients $m_i, i = 0, 1, 2, 3$ and $m_1(m_2m_3 - m_1) - m_3^2m_0$ are all positive. Clearly, it can be seen from Eq. 13 that $m_3 > 0, m_2 > 0, m_1 > 0$ and $m_0 > 0$ if $R_0 < 1$. This implies that $R_{0A} < 1$ and $R_{0A} + R_{0I} < 1$ since R_0 is the sum of R_{0A}, R_{0I} and R_{0H}. Intuitively, it follows that the disease-free equilibrium D_0 is locally asymptotically stable provided $m_1(m_2m_3 - m_1) - m_3^2m_0$ is strictly positive. Otherwise unstable. □

3.3. Threshold analysis

To assess the impact of inhibition factor η_1 adopted by susceptible, exposed and asymptomatic individuals, hospitalization of individuals with COVID-9 symptoms (h), treatment rate (γ) and denial rate (d) of COVID-19, we compute the partial derivatives of R_0 with respect to η_1, h, γ and d as presented below:

$$\begin{aligned} \frac{\partial R_0}{\partial \eta_1} &= -\Big(\frac{\sqrt{\beta}S_0}{(1+(\eta_1-d)S_0)}\Big)^2\Big(\frac{\rho_1c_1}{\sigma_1\sigma_2} + \frac{\rho_2\rho_1c_2}{\sigma_1\sigma_2\sigma_3} + \frac{h\rho_2\rho_1c_3}{\sigma_1\sigma_2\sigma_3\sigma_4}\Big), \\ \frac{\partial R_0}{\partial h} &= \frac{\beta S_0}{(1+(\eta_1-d)S_0)}\Big(\frac{(\mu+\delta)c_3 - (\mu+\delta+\gamma)c_2}{(\mu+\rho_1)(\mu+\nu+\rho_2)(\mu+\delta+\gamma)(\mu+\delta+h)^2}\Big), \\ \frac{\partial R_0}{\partial \gamma} &= -\frac{\beta S_0}{(1+(\eta_1-d)S_0)}\Big(\frac{h\rho_2\rho_1c_3}{(\mu+\rho_1)(\mu+\nu+\rho_2)(\mu+\delta+h)(\mu+\delta+\gamma)^2}\Big), \\ \frac{\partial R_0}{\partial d} &= \Big(\frac{\sqrt{\beta}S_0}{(1+(\eta_1-d)S_0)}\Big)^2\Big(\frac{\rho_1c_1}{\sigma_1\sigma_2} + \frac{\rho_2\rho_1c_2}{\sigma_1\sigma_2\sigma_3} + \frac{h\rho_2\rho_1c_3}{\sigma_1\sigma_2\sigma_3\sigma_4}\Big). \end{aligned}$$

From the above analysis, we observe that $\frac{\partial R_0}{\partial \eta_1} < 0$, $\frac{\partial R_0}{\partial \gamma} < 0$, $\frac{\partial R_0}{\partial h} < 0$ if $(\mu+\delta)c_3 < (\mu+\delta+\gamma)c_2$ and $\frac{\partial R_0}{\partial d} > 0$. The last inequality clearly explains that the denial of COVID-19 existence will heavily contribute to the rapid spread of the virus and challenged the process of the disease prevention. The first three inequalities show that inhibition factors, hospitalization and treatment by Holling type II curtail the outgrowing cases of COVID-19 pandemic.

It is also invaluable to determine the upper bounds for infection and denial rates as well as the lower bound for inhibition factors.

If

$$R_0 = \frac{\beta S_0 \Omega}{1 + (\eta_1 - d)S_0} < 1,$$

$$\text{with} \quad \Omega = \frac{\rho_1 c_1}{\sigma_1 \sigma_2} + \frac{\rho_2 \rho_1 c_2}{\sigma_1 \sigma_2 \sigma_3} + \frac{h\rho_2 \rho_1 c_3}{\sigma_1 \sigma_2 \sigma_3 \sigma_4},$$

then,

$$\beta < \frac{1 + (\eta_1 - d)S_0}{\beta S_0 \Omega}, d < \frac{1}{S_0} + \eta_1 (1 - \frac{\beta \Omega}{\eta_1})$$

and the lower bound for η_1 is:

$$\eta_1 > -\frac{1}{S_0} + d + \beta \Omega.$$

Using the values in Table 1, we obtain the Figures SM1 and SM2.

3.4. Existence of endemic equilibria and backward bifurcation

Before assessing the global asymptotic dynamics of the DFE, it is important to find number of equilibrium solutions of system 5. To do so, we can set the right hand sides of System 5 to zero (at steady state) to arrive at the following expressions for the endemic equilibrium point (EEP), $D_*(S_*, E_*, A_*, I_*, H_*)$ as:

$$\begin{aligned}
S_* &= \frac{\hat{B}h\rho_2\rho_1(1 + \epsilon H_*) - \sigma_1\sigma_2\sigma_3(\gamma + q + q\epsilon H_*)H_*}{\mu h\rho_2\rho_1(1 + \epsilon H_*)}, \\
E_* &= \frac{\sigma_2\sigma_3(\gamma + q + q\epsilon H_*)H_*}{h\rho_2\rho_1(1 + \epsilon H_*)}, \\
A_* &= \frac{\sigma_3(\gamma + q + q\epsilon H_*)H_*}{h\rho_2(1 + \epsilon H_*)}, \\
I_* &= \frac{(\gamma + q + q\epsilon H_*)H_*}{h(1 + \epsilon H_*)},
\end{aligned}$$

and H_* is the root of the following cubic polynomial equation

$$PH_*^3 + QH_*^2 + RH_* + U = 0, \tag{14}$$

where

$$\begin{aligned}
P &= \sigma_1\sigma_2\sigma_3 q^2\epsilon^2[\sigma_2\sigma_3(\eta_1 - d)(\nu + \rho_1) + \mu\rho_1(\sigma_3(\eta_1 - d) + \rho_2\eta_2 + h\rho_2\eta_3)] \\
&\quad + \beta\sigma_1\sigma_2\sigma_3 q\epsilon^2\rho_1(\sigma_3 q c_1 + \rho_2 q c_2 + h\rho_2 c_3), \\
Q &= Q_1 - Q_2, \\
R &= \sigma_1\sigma_2\sigma_3 h\rho_2\rho_1\epsilon(\gamma + q)(\mu + (\eta_1 - d)\hat{B})(1 - R_0) - h\rho_2\rho_1 q\epsilon[Q_3 - Q_4], \\
U &= \sigma_1\sigma_2\sigma_3 h\rho_2\rho_1(\gamma + q)(\mu + (\eta_1 - d)\hat{B})(1 - R_0),
\end{aligned} \tag{15}$$

with

$$\begin{aligned}
Q_1 &= \frac{2\sigma_1^2\sigma_2^2\sigma_3^2 q\epsilon^2}{\hat{B}}(\gamma + q)(\mu + (\eta_1 - d)\hat{B})R_0 + 2\sigma_1\sigma_2\sigma_3\mu\rho_1\epsilon(\gamma + q)(\sigma_3 q(\eta_1 - d) + q\rho_2\eta_2 + h\rho_2\eta_3) \\
&\quad + \sigma_1\sigma_2\sigma_3 h\rho_2\rho_1\epsilon(\beta\gamma c_3 + q\epsilon(\mu + (\eta_1 - d)\hat{B})), \\
Q_2 &= \mu\sigma_1\sigma_2\sigma_3 h\rho_2\rho_1\epsilon\gamma\eta_3 + 2\sigma_1\sigma_2^2\sigma_3^2 q\epsilon(\eta_1 - d)(\nu + \rho_1)(\gamma + q) \\
&\quad + \beta\hat{B}hq^2\rho_2\rho_1^2(\sigma_3 q c_1 + \rho_2 q c_2 + h\rho_2 c_3), \\
Q_3 &= \beta\hat{B}\rho_1(\sigma_3 q c_1 + \rho_2 q c_2 + h\rho_2 c_3), \\
Q_4 &= h\rho_2\rho_1(\mu + (\eta_1 - d)\hat{B}) \quad \text{and} \\
q &= \mu + \delta.
\end{aligned}$$

It is obvious from Eq. 15 that $P > 0$ (since all the parameters of the model are non-negative with $0 \leq d < \eta_1$) and $U > 0$ provided that $R_0 < 1$. Therefore, the number of possible positive roots of Eq. 14 can depends on the signs of Q and R. Following the work of Gumel and Sharomi [33], this can be analyzed using the Descarte's rule of signs on the cubic $g(x) = Px^3 + Qx^2 + Rx + U$, given Eq. 14 (with $x = H_*$). The results (Theorem 3.2 and Conjuncture 1) below follow from the various cases listed in Table 2.

Theorem 3.2. *The COVID-19 Model 5*

Table 1
Variables and parameters of the model .

Variables	Description	Value	Ref.
$S(t)$	Number of Susceptible individuals at time, t	200×10^6	[18]
$E(t)$	Number of Exposed individuals at time, t	1565	[Assumed]
$A(t)$	Number of Asymptomatic individuals at time, t	80	[Assumed]
$I(t)$	Number of Symptomatic individuals at time, t	20	[Assumed]
$H(t)$	Number of Hospitalized individuals at time, t	10	[Assumed]
$R(t)$	Number of Recovered individuals at time, t	0	[Assumed]
Parameters	Description	Value	Ref.
$\hat{B}$	Recruitment rate into Susceptible individuals	22655	[18]
β	Infection rate	0.05	[Assumed]
η_1, η_2, η_3	Inhibition factors	0.55,0.3,0.5	[Assumed]
c_1, c_2, c_3	Contact rates of susceptibles with A, I and H respectively	0.5,0.3,0.1	[Assumed]
d	Rate of the denial of the disease	[0,0.4)	[Assumed]
μ	Natural death rate	0.0182	[18]
γ	Maximum treatment rate of the hospitalized individuals	1/15	[18]
ν	Rate of recovery of the asymptomatic individuals	1/7	[29]
δ	Disease induced death rate	0.022	[18]
ϵ	Reduced transmission factor of recovered individuals	0.5	[Assumed]
h	Rate of hospitalization of Symptomatic individuals	0.025	[29]
ρ_1	Rate of progression from E to A individuals	1/5.1	[29]
ρ_2	Rate at which individuals in A develop symptoms	1/7	[18]

Table 2
Number of possible positive real roots of $g(x)$ for $R_0 < 1$ and $R_0 > 1$.

Cases	P	Q	R	U	R_0	No. of sign changes	No. of endemic Points
1	+	+	+	+	$R_0 < 1$	0	0
	+	+	+	-	$R_0 > 1$	1	1
2	+	-	-	+	$R_0 < 1$	2	0, 2
	+	-	-	-	$R_0 > 1$	1	1
3	+	+	-	+	$R_0 < 1$	2	0, 2
	+	+	-	-	$R_0 > 1$	1	1
4	+	-	+	+	$R_0 < 1$	2	0, 2
	+	-	+	-	$R_0 > 1$	3	1, 3

(a) *has a unique endemic equilibrium point if $R_0 > 1$ and whenever the cases 1, 2 and 3 are satisfied;*
(b) *could have at least one endemic equilibrium point if $R_0 > 1$ and case 4 is satisfied;*
(c) *could have at least two endemic equilibria if $R_0 < 1$ and cases 2–4 are satisfied.*

Conjuncture 1. The COVID-19 Model 5 has more than one positive endemic equilibrium point when $R_0 > 1$ and could have zero or two positive equilibria when $R_0 < 1$.

The occurrence of multiple endemic equilibria at $R_0 < 1$ (as indicated in Table 2) suggests the likelihood of backward bifurcation (see [33]), where the stable DFE co-exists with a stable endemic equilibrium point(EEP), in a scenario when the basic reproduction number is below unity. This is explored via numerical simulations (rigorous result can be obtained using centre manifold theory (see [34]) as illustrated in the Fig. 2 and Figure SM3. Fig. 2 depicts the associated backward bifurcation diagram. Furthermore Figure SM3 shows convergence to both the DFE and the EEP for the total asymptomatic and symptomatic individuals when $R_0 < 1$ depending on the initial sizes of the sub-populations. The biological consequence of this result is that the effective control of COVID-19 in a population (when $R_0 < 1$) is independent on the initial sizes of the sub-populations of the Model 5 within the bounds of denial rate.

4. Global analysis

Theorem 4.1. *The COVID-19-free equilibrium D_0 is globally asymptotically stable if $R_0 < 1$.*

Proof. The work of Naji and Abdulateef [14] is the basis by which this theorem can be verified. Adopting a similiar real-valued function

$$L_0 = \frac{(S - S_0)^2}{2} + E + A + I + H$$

with the derivative

$$L_0^{'}(t) = (S - S_0)\frac{dS}{dt} + \frac{dE}{dt} + \frac{dA}{dt} + \frac{dI}{dt} + \frac{dH}{dt}. \tag{16}$$

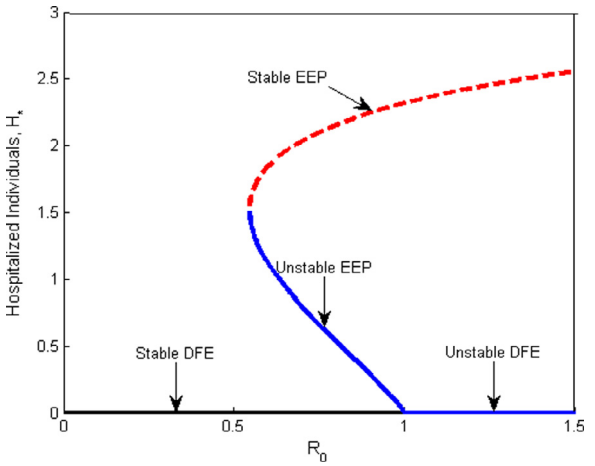

Fig. 2. Bifurcation diagram for the Model 5. Parameter values used are: $\beta = 0.009, \hat{B} = 180, \quad \delta = 0.8$ and $d = 0.51$ (so that $R_{0A} = 0.3378752329, R_{0I} = 0.03434622182, R_{0H} = 0.0003234594838$ and $R_0 = 0.3725449142$). All other parameter values are in Table 1. It is essential to note that the values of the parameters were used for illustrative purpose only, and may not be realistic epidemiologically.

Upon substitution of System 5 in Eq. 16, we have

$$\begin{aligned} L_0^{'}(t) &= (S - S_0)(\hat{B} - \bar{f}S - \mu S) + (\bar{f}S - (\mu + \rho_1)E) + (\rho_1 E - (\mu + \nu + \rho_2)A) \\ &\quad + (\rho_2 A - (\mu + \delta + h)I) + (hI - \bar{g}(H) - (\mu + \delta)H). \end{aligned}$$

Taking $\hat{B} = \mu S_0$, we obtain

$$\begin{aligned} L_0^{'}(t) &= -\mu(S - S_0)^2 - \bar{f}S^2 + (1 + S_0)\bar{f}S - \mu E - (\mu + \nu)A - (\mu + \delta)I \\ &\quad - \Big(\mu + \delta + \frac{\gamma}{1 + \epsilon H}\Big)H \\ &\leq -\mu(S - S_0)^2 + (1 + S_0)\Big(\frac{\beta(c_1 A + c_2 I + c_3 H)}{1 + (\eta_1 - d)(S + E + A) + \eta_2 I + \eta_3 H}\Big)S \\ &\quad - (\mu + \nu)A - (\mu + \delta)I - \Big(\mu + \delta + \frac{\gamma}{1 + \epsilon H}\Big)H \end{aligned}$$

If $\bar{a} = min(\eta_1 - d, \eta_2, \eta_3, \eta_4) = \eta_1 - d$ (by assumption), then

$$\begin{aligned} L_0^{'}(t) &= -\mu(S - S_0)^2 - \bar{f}S^2 + (1 + S_0)\bar{f}S - \mu E - (\mu + \nu)A - (\mu + \delta)I \\ &\quad - \Big(\mu + \delta + \frac{\gamma}{1 + \epsilon H}\Big)H \\ &\leq -\mu(S - S_0)^2 + (1 + S_0)\Big(\frac{\beta(c_1 A + c_2 I + c_3 H)}{1 + \bar{a}N}\Big)S \\ &\quad - (\mu + \nu)A - (\mu + \delta)I - \Big(\mu + \delta + \frac{\gamma}{1 + \epsilon H}\Big)H. \end{aligned}$$

But, $N(t) \leq \frac{\hat{B}}{\bar{\mu}}, S(t) \leq \frac{\hat{B}}{\mu}$ and $S_0 = \frac{\hat{B}}{\mu}$

$$\begin{aligned} L_0^{'}(t) \quad &\leq -\mu(S - S_0)^2 - (\mu + \nu)\Big(1 - \tfrac{\beta c_1 S_0(\mu + \hat{B})}{(\mu + \bar{a}\hat{B})(\mu + \nu)}\Big)A - (\mu + \delta)\Big(1 - \tfrac{\beta c_2 S_0(\mu + \hat{B})}{(\mu + \bar{a}\hat{B})(\mu + \delta)}\Big)I \\ &\quad -(\mu + \delta + \tfrac{\gamma}{1 + \epsilon H})\Big(1 - \tfrac{\beta c_3 S_0(\mu + \hat{B})}{(\mu + \bar{a}\hat{B})(\mu + \delta + \frac{\gamma}{1 + \epsilon H})}\Big)H. \end{aligned} \tag{17}$$

Now replacing $\beta c_1 S_0, \beta c_2 S_0$ and $\beta c_3 S_0$ in terms of R_0 into Eq. 17, we have

$$\begin{aligned} L_0^{'}(t) &\leq -\mu(S - S_0)^2 - (\mu + \nu)\Big(1 - R_{0A}\frac{(\mu + \hat{B})}{(\mu + \bar{a}\hat{B})(\mu + \nu)}\Big)A - (\mu + \delta)\Big(1 - R_{0I}\frac{(\mu + \hat{B})}{(\mu + \bar{a}\hat{B})(\mu + \delta)}\Big)I \\ &\quad - (\mu + \delta + \frac{\gamma}{1 + \epsilon H})\Big(1 - R_{0H}\frac{(\mu + \hat{B})}{(\mu + \bar{a}\hat{B})(\mu + \delta + \frac{\gamma}{1 + \epsilon H})}\Big)H. \end{aligned}$$

Therefore, $L_0^{'}(t) < 0$ if $R_{0A} < 1, R_{0I} < 1, R_{0H} < 1$ implying that $R_0 < 1$ and $L_0^{'}(t) = 0$ if $A = I = H = 0$ and $S = S_0 = \frac{\hat{B}}{\mu}$.

We conclude that the largest compact invariant set in $\{(S, E, A, I, H) \in \hat{\psi} : L_0^{'}(t) = 0\}$ is the only set $\{D_0\}$. By La Salle's invariance principle [35], the COVID-19-free equilibrium is globally asymptotically stable if $R_0 < 1$ □

The time series plots showing the number of exposed, asymptomatic, symptomatic and hospitalized people when the condition $R_0 < 1$ in the above theorem is given by Figure SM4.

Theorem 4.2. *The endemic equilibrium point D_* is globally asymptotically stable if $R_0 > 1$ and $\gamma = 0$.*

Proof. Using the work in [36], let $\lambda(I) = (C_1A + C_2I + C_3H)\Psi(I)$, and $\Psi(H) = \frac{1}{1+\epsilon H}$, where $\Psi(I) = \frac{1}{1+(\eta_1-d)(S+E+A)+\eta_2 I+\eta_3 H}$

Then, we adopt the following Lyapunov function

$$\begin{aligned} L(x) \quad &= (S - S_* - S_* \ln \tfrac{S}{S_*}) + (E - E_* - E_* \ln \tfrac{E}{E_*}) + \tfrac{\lambda(I_*)\beta S_*}{\rho_1 E_*}(A - A_* - A_* \ln \tfrac{A}{A_*}) \\ &+ \tfrac{\lambda(I_*)\beta S_*}{\rho_2 A_*}(I - I_* - I_* \ln \tfrac{I}{I_*}) + \tfrac{\lambda(I_*)\beta S_*}{hI_*}(H - H_* - H_* \ln \tfrac{H}{H_*}). \end{aligned} \tag{18}$$

Putting System 5 into the derivative of the Lyapunov function in Eq. 18 gives

$$\begin{aligned} L' \quad &= (1 - \tfrac{S_*}{S})\Big(\hat{B} - \lambda(I)\beta S - \mu S\Big) + (1 - \tfrac{E_*}{E})\Big(\lambda(I)\beta S - (\mu + \rho_1)E\Big) \\ &+ \tfrac{\lambda(I_*)\beta S_*}{\rho_1 E_*}(1 - \tfrac{A_*}{A})\Big(\rho_1 E - (\mu + \nu + \rho_2)A\Big) + \tfrac{\lambda(I_*)\beta S_*}{\rho_2 A_*}(1 - \tfrac{I_*}{I})\Big(\rho_2 A - (\mu + \delta + h)I\Big) \\ &+ \tfrac{\lambda(I_*)\beta S_*}{hI_*}(1 - \tfrac{H_*}{H})\Big(hI - \gamma H\Psi(H) - (\mu + \delta)H\Big). \end{aligned} \tag{19}$$

At equilibrium state

$$\hat{B} = \lambda(I_*)\beta S_* + \mu S_*, \mu + \rho_1 = \frac{\lambda(I_*)\beta S_*}{E_*}, \mu + \nu + \rho_2 = \frac{\rho_1 E_*}{A_*},$$

$$\mu + \delta + h = \frac{\rho_2 A_*}{I_*}, \mu + \delta = \frac{hI_*}{H_*} - \gamma\Psi(H_*).$$

Expanding Eq. 19 at endemic equilibrium point and after simplifying, we get

$$\begin{aligned} L' = \mu S_*(2 - \frac{S_*}{S} - \frac{S}{S_*}) + \beta S_*\lambda(I_*)\Big[5 + \frac{\lambda(I)}{\lambda(I_*)} - \frac{S_*}{S} - \frac{S}{S_*}\frac{E_*}{E}\frac{\lambda(I)}{\lambda(I_*)} - \frac{E}{E_*}\frac{A_*}{A} - \frac{A}{A_*}\frac{I_*}{I} \\ - \frac{H}{H_*} - \frac{I}{I_*}\frac{H_*}{H}\Big] + \frac{\lambda(I_*)\beta S_*}{hI_*}\gamma H_*\Psi(H_*)\Big[-1 + \frac{H}{H_*} - \frac{H}{H_*}\frac{\Psi(H)}{\Psi(H_*)} + \frac{\Psi(H)}{\Psi(H_*)}\Big] \end{aligned}$$

But, setting $\gamma = 0$ and $\frac{\lambda(I)}{\lambda(I_*)} \leq 1$, since $\lambda(I)$ is an increasing function, we have

$$L' = \mu S_*(2 - \frac{S_*}{S} - \frac{S}{S_*}) + \beta S_*\lambda(I_*)\Big[6 - \frac{S_*}{S} - \frac{S}{S_*}\frac{E_*}{E} - \frac{E}{E_*}\frac{A_*}{A} - \frac{A}{A_*}\frac{I_*}{I} - \frac{H}{H_*} - \frac{I}{I_*}\frac{H_*}{H}\Big]$$

By arithmetic-geometric theorem,

$$2 \leq \frac{S_*}{S} + \frac{S}{S_*}, \quad 6 \leq \frac{S_*}{S} + \frac{S}{S_*}\frac{E_*}{E} + \frac{E}{E_*}\frac{A_*}{A} + \frac{A}{A_*}\frac{I_*}{I} + \frac{H}{H_*} + \frac{I}{I_*}\frac{H_*}{H}$$

.

Therefore, $L' \leq 0$. Hence, the System 5 is globally asymptotically stable if $R_0 > 1$ by La Salle invariance principle. □

The biological significance of the above result is that, in the absence of maximum treatment for the hospitalized people ($\gamma = 0$), COVID-19 pandemic will not be eliminated from the community if the basic reproduction number, R_0 rise above unity.

5. Optimal control analysis

In this section, we denote mathematically the three time series controls as $\xi_1(t), \xi_2(t) = h(t)$ and $\xi_3(t) = \gamma(t)$ for $t \in [0, t_f]$, where t_f is the time period of the intervention to represent the additional preventive protocol(creation of awareness about COVID-19) for the susceptible and exposed, testing and isolation (hospitalization) and treatment interventions. The application of preventive protocol reduces the force of COVID-19 infection as modelled in Eq. 20

$$\bar{f}_0(t) = \frac{\beta(1 - \xi_1(t))(c_1A + c_2I + c_3H)}{1 + (\eta_1 - d)(S + E + A) + \eta_2 I + \eta_3 H}. \tag{20}$$

The testing boost the chances of hospitalization and medical care of the infected people while treatment program may lead to their recovery. Our main motive which is to minimize the number of COVID-19 cases and the cost of control measures involved, can be mathematically translated into finding piecewise continuous controls $\xi_1^*, \xi_2^*, \xi_3^*$ and associated state variables S^*, E^*, A^*, I^*, H^* and R^* that minimize the objective functional J given by Eq. 21

$$J(\xi_1^*, \xi_2^*, \xi_3^*) = \int_0^{t_f} \Big(kE + pA + qI + rH + \frac{m_1}{2}\xi_1^2 + \frac{m_2}{2}\xi_2^2 + \frac{m_3}{2}\xi_3^2\Big)\, dt, \tag{21}$$

where $m_i > 0$ for $i = 1, 2, 3$ weighs constants that balance the optimal controls. The terms $m_1\xi_1^2, m_2\xi_2^2$ and $m_3\xi_3^2$ are the cost associated with preventive protocols for susceptible and exposed, testing and hospitalization for symptomatic individuals

and attaining maximum treatment for hospitalized, respectively. Therefore, greater values of m_1, m_2 and m_3 will indicate higher implementation costs for the preventive protocols, testing and hospitalization and maximum treatment for COVID-19, respectively. The above terms are assumed non-linear and quadratic due to denial in observing preventive protocols, cost of testing and hospitalizing symptomatic individuals and achieving maximum treatment for the hospitalized individuals.

Optimal control problem is to minimize the objective functional subject to the non-linear system in Eq. 22

$$\begin{aligned}
\frac{dS}{dt} &= \hat{B} - \bar{f}_0(t)S - \mu S,\\
\frac{dE}{dt} &= \bar{f}_0(t)S - (\mu+\rho_1)E,\\
\frac{dA}{dt} &= \rho_1 E - (\mu+\nu+\rho_2)A,\\
\frac{dI}{dt} &= \rho_2 A - (\mu+\delta+\xi_2(t))I,\\
\frac{dH}{dt} &= \xi_2(t)I - \frac{\xi_3(t)H}{1+\epsilon H} - (\mu+\delta)H,\\
\frac{dR}{dt} &= \nu A + \frac{\xi_3(t)H}{1+\epsilon H} - \mu R.
\end{aligned} \tag{22}$$

We set the optimal controls ξ_i^*, ξ_2^* and ξ_3^* such that

$$J(\xi_i^*, \xi_2^*, \xi_3^*) = \underbrace{min}_{\nabla} J(\xi_i, \xi_2, \xi_3), \tag{23}$$

where $\nabla = \{(\xi_i, \xi_2, \xi_3) | 0 \leqslant \xi_i(t) \leqslant 1, i = 1, 2, 3\}$ is the set for the controls.

Remark 1. In this set ∇, when the rate of a control is zero, then no investment in control has been made. On the other hand, when the value of a control is one, then a control effort has been achieved maximally.

At this point, we employ the Pontryagin's maximum principle to obtain the necessary conditions for getting optimal controls ξ_i^*, ξ_2^* and ξ_3^* that satisfy Eq. 23 with constraint model in Eq. 22. The principle converts Eqs. 21 - 23 into a minimization problem of Hamiltonian function $\bar{H_\alpha}$ in terms of (ξ_i, ξ_2, ξ_3)

$$\bar{H_\alpha} = kE(t) + pA(t) + qI(t) + rH(t) + \sum_{i=1}^{3} \frac{m_i}{2}\xi_i^2(t) + \sum_{i=1}^{6} \zeta_i g_i,$$

where g_i denote the ith right side in Eq. 22 and ζ_i is the ith adjoint that satisfy the co-state functions given in Eq. 24

$$\begin{aligned}
\zeta_1' &= -\frac{\partial \bar{H_\alpha}}{\partial S} = (\zeta_1 - \zeta_2)\beta(1-\xi_1(t))\left(\frac{L_1 L_2}{T^2}\right) + \mu\zeta_1,\\
\zeta_2' &= -\frac{\partial \bar{H_\alpha}}{\partial E} = -k + (\zeta_2 - \zeta_1)\beta(1-\xi_1(t))(\eta_1 - d)S\left(\frac{L_1}{T^2}\right) + (\zeta_2 - \zeta_3)\rho_1 + \mu\zeta_2,\\
\zeta_3' &= -\frac{\partial \bar{H_\alpha}}{\partial A} = -p + (\zeta_1 - \zeta_2)\beta(1-\xi_1(t))S\left(\frac{L_3}{T^2}\right) + (\zeta_3 - \zeta_4)\rho_2 + (\zeta_3 - \zeta_6)\nu + \mu\zeta_3,\\
\zeta_4' &= -\frac{\partial \bar{H_\alpha}}{\partial I} = -q + (\zeta_1 - \zeta_2)\beta(1-\xi_1(t))S\left(\frac{L_4}{T^2}\right) + (\zeta_4 - \zeta_5)\xi_2(t) + (\mu+\delta)\zeta_4,\\
\zeta_5' &= -\frac{\partial \bar{H_\alpha}}{\partial H} = -r + (\zeta_1 - \zeta_2)\beta(1-\xi_1(t))S\left(\frac{L_5}{T^2}\right) + (\zeta_5 - \zeta_6)\frac{\xi_3(t)}{(1+\epsilon H)^2} + (\mu+\delta)\zeta_5,\\
\zeta_6' &= -\frac{\partial \bar{H_\alpha}}{\partial R} = \mu\zeta_6,
\end{aligned} \tag{24}$$

where

$$L_1 = c_1A^* + c_2I^* + c_3H^*, L_2 = 1 + (\eta_1 - d)(E^* + A^*) + \eta_2 I^* + \eta_3 H^*$$

$$L_3 = c_1(1 + (\eta_1 - d)(S^* + E^*)) + (\eta_2 c_1 - (\eta_1 - d)c_2)I^* + (\eta_3 c_1 - (\eta_1 - d)c_3)H^*$$

$$L_4 = c_2(1 + (\eta_1 - d)(S^* + E^*)) + ((\eta_1 - d)c_2 - \eta_2 c_1)A^* + (\eta_3 c_2 - \eta_2 c_3)H^*$$

$$L_5 = c_3(1 + (\eta_1 - d)(S^* + E^*)) + ((\eta_1 - d)c_3 - \eta_3 c_1)A^* + (\eta_2 c_3 - \eta_3 c_2)I^*$$

$$T = 1 + (\eta_1 - d)(S^* + E^* + A^*) + \eta_2 I^* + \eta_3 H^*$$

and final time conditions $\zeta_i(t_f) = 0, i = 1, 2, \ldots, 6$.

The procedure for obtaining the optimal controls $\xi = (\xi_i^*, \xi_2^*, \xi_3^*)$ are mentioned below [37].

Step 1. Minimize the Hamiltonian function $\bar{H_\alpha}$ with respect to ξ, we get

$$\xi_1^* = \begin{cases} 0, & \text{if} \quad \xi_1 \leqslant 0 \\ \frac{(\zeta_2 - \zeta_1)\beta(c_1A^* + c_2I^* + c_3H^*)}{m_1(1 + (\eta_1 - d)(S^* + E^* + A^*) + \eta_2 I^* + \eta_3 H^*)}, & \text{if} \quad 0 < \xi_1 < 1 \\ 1, & \text{if} \quad \xi_1 \geqslant 1 \end{cases}$$

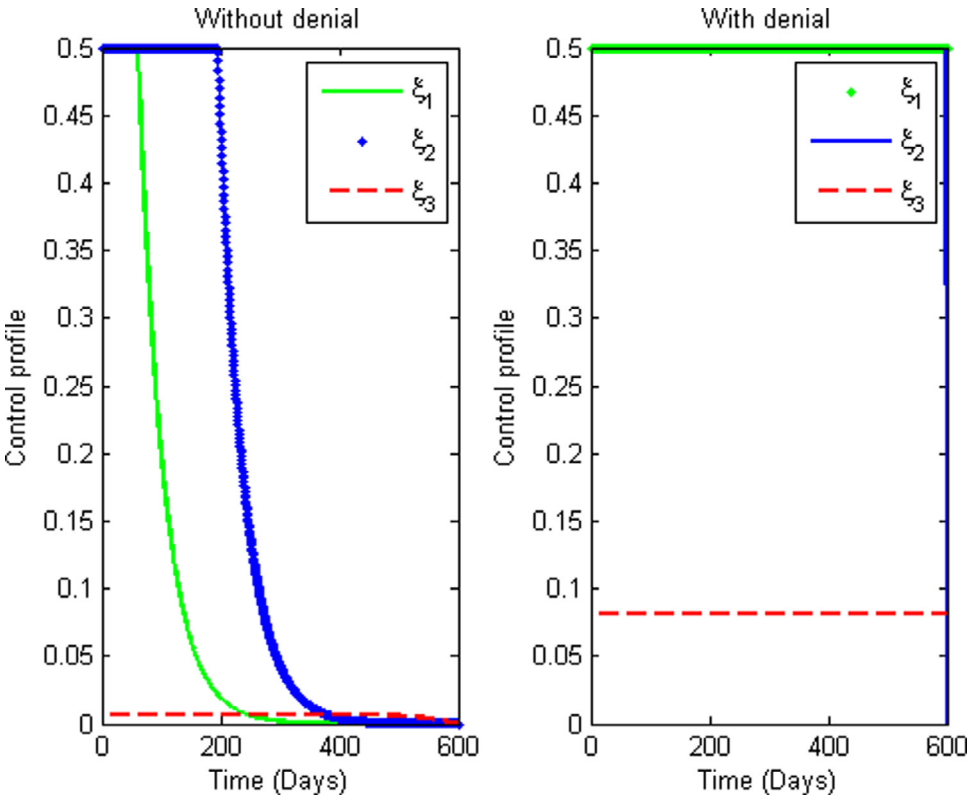

Fig. 3. Profile of optimal controls, ξ_1^*, ξ_2^* and ξ_3^*, when $d = 0$ (Figure on the left) and $d = 0.55$ (Figure on the right). Parameter values are as given in Table 1.

$$\xi_2^* = \begin{cases} 0, & \text{if} \quad \xi_2 \leqslant 0 \\ \frac{(\zeta_4 - \zeta_5)I^*}{m_2}, & \text{if} \quad 0 < \xi_2 < 1 \\ 1, & \text{if} \quad \xi_2 \geqslant 1 \end{cases}$$

$$\xi_3^* = \begin{cases} 0, & \text{if} \quad \xi_3 \leqslant 0 \\ \frac{(\zeta_5 - \zeta_6)H^*}{m_3(1+\epsilon H^*)}, & \text{if} \quad 0 < \xi_3 < 1 \\ 1, & \text{if} \quad \xi_3 \geqslant 1 \end{cases}$$

Step 2. Obtain the solutions of the system $\frac{dx}{dt} = \frac{\partial \bar{H}_\alpha}{\partial \zeta}$, where $x = (S, E, A, I, H, R)$, $\zeta = (\zeta_1, \zeta_2, \ldots, \zeta_6)$ using the initial condition $x_0 = (S(0), E(0), A(0), I(0), H(0), R(0))$.

Step 3. Determine the solution of the co-state system $\frac{d\zeta}{dt} = -\frac{\partial \bar{H}_\alpha}{\partial x}$ with the final time conditions $\zeta_i(t_f) = 0$, $i = 1, 2, \ldots, 6$.

In line with the above procedure, the optimal control $(\xi_i^*, \xi_2^*, \xi_3^*)$ is given in the next theorem.

Theorem 5.1. *The optimal controls $(\xi_i^*, \xi_2^*, \xi_3^*)$ that minimizes the cost function $J(\xi_i, \xi_2, \xi_3)$ on $\triangledown$ subject to the system in Eq. 22 is:*

$$\xi_1^* = max\left\{0, min\left\{1, \frac{(\zeta_2 - \zeta_1)\beta(c_1A^* + c_2I^* + c_3H^*)}{m_1(1 + (\eta_1 - d)(S^* + E^* + A^*) + \eta_2 I^* + \eta_3 H^*)}\right\}\right\},$$

$$\xi_2^* = max\left\{0, min\left\{1, \frac{(\zeta_4 - \zeta_5)I^*}{m_2}\right\}\right\},$$

$$\xi_3^* = max\left\{0, min\left\{1, \frac{(\zeta_5 - \zeta_6)H^*}{m_3(1 + \epsilon H^*)}\right\}\right\},$$

where $\zeta_i, i = 1, 2, \ldots, 6$ remain the solutions of the co-state system in Eq. 24.

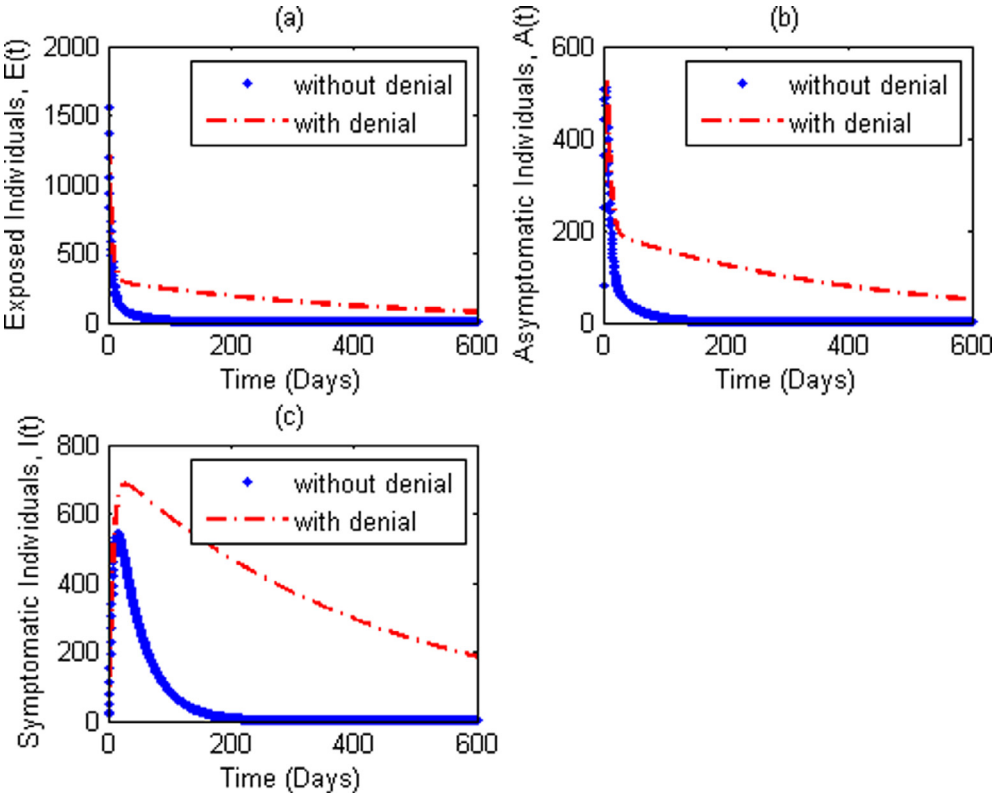

Fig. 4. The population dynamics of (a) Exposed, (b) Asymptomatic and (c) Symptomatic individuals to COVID-19 using optimal controls, ξ_1^*, ξ_2^* and ξ_3^*, with denial effect. Parameter values are as given in Table 1.

6. Numerical results and discussions

In this section, numerical simulations are carried out using the parameters values in Table 1. We make the comparison of the optimal control system in Eq. 22 in terms of denial and without denial. The fourth-order Runge-Kutta (RK4) scheme is employed to solve the optimal control strategy; and adopted the forward RK4 scheme and backward RK4 scheme to solve the state system and co-state system, respectively. Apart from the initial conditions and other parameters values given in Table 1, we take $m_3 = 50, m_2 = 30$ and $m_1 = 15$ since the cost of treating hospitalized people is higher than the cost of isolating symptomatic people which in turn is higher than the cost of protecting susceptible. We also consider $k = p = 0.1, q = 0.15$ and $r = 0.015$ for the numerical simulations.

It is evident from Figure SM1 that cases of COVID-19 grow exponentially in the population when denial rate exceeds 0.45 since $R_0 > 1$. However, when d satisfy the inequality $0 \leq d < 0.45$, $R_0 < 1$ and the disease can be curtailed. Figure SM2 displays the level set of R_0 in β and d planes. They show that the number of cases of COVID-19 increases as d increases. This implies that with denial: preventable strategies, hospitalization and treatment measures may not be enough for crumbing COVID-19.

The profile of the optimal controls $\xi_1^*, \xi_2^*, \xi_3^*$ is given by Fig. 3. Implementation of this strategy without denial, COVID-19 prevention, hospitalization and treatment of symptomatic individuals should be done intensively for almost 50, 200 and 600 days, respectively, and then decline to the lower bound. However, with denial we observed from the graph on the right in Fig. 3 that each control needed to be applied seriously for 600 days. Likewise, Fig. 4 shows that each population; Exposed, Asymptomatic and Symptomatic has been reduced successfully without the denial of the disease. On the other hand, denial of the pandemic has rendered these controls ineffective since the number of infectives Asymptomatic, Symptomatic and the exposed persist uniformly. This means that control in the presence of denial cannot eliminate the ongoing COVID-19 pandemic. This result is consistent with the outcome of the work by Sayedahmed et al. [26] that says good level of knowledge (awareness creation) is associated with good practice towards COVID-19 elimination. The outcome is also in line with the report on the effect of denial on other diseases like HIV/AIDS [10,11] that says denial triggers the spread of HIV/AIDS. We observed from Figure SM4 that in the presence of maximum treatment and preventive protocols (i.e. use of face masks, hand sanitizers, social distancing) with out denial actually reduced the number of COVID-19 cases recorded against exposed, asymptomatic, symptomatic and hospitalized people. This result coincides with the work of Deressa and Duressa [28] that emphasises that public health education, protective measures and treatment of hospitalized are effective to significantly

decrease the number of COVID-19 cases among the infected population. Furthermore, We display in Figure SM5 the necessity of time in eradicating COVID-19 in the population. These figures show that the number of Exposed, Asymptomatic and Symptomatic individuals (E(t), A(t), I(t)) will decrease drastically when the controls are time-dependent compare to when the controls are constant (do not dependent on time). This implies that even when tested control strategies are in place, it is crucial to implement them on time in order to gain effective outcome. For instance, hospitalization of Symptomatic individuals on time will prevent them from infecting susceptible individuals while treating them urgently will avert deaths that could have been recorded. This conforms to the result of Madubueze et al. [38] that says time dependent interventions reduced the number of exposed and infected individuals compared to constant interventions. From our findings, we conclude that people should accept the fact that COVID-19 exists, and take necessary preventive protocols, and maximum treatment for the hospitalized people. Since human altitude towards disease outbreak can not completely changed, the denial rate of COVID-19 existence should be less than 0.45 in order to control the spread of the pandemic.

7. Conclusion

In this paper, we assess the role of denial on the spread of COVID-19 pandemic through the construction of an optimal control model with Beddington-De Angelis incidence function. From our analyzes, we derived the control reproduction number that determines the existence and stability of the model equilibria. Also, we found that to put the pandemic under control, the infection and denial rates should not exceed the upper bounds 0.15 and 0.45 on average. By implication, the disease will continue to live with us if 45 people in every 100 deny the existence of the disease. The presence of denial rate in the system induces backward bifurcation that causes complexity in the disease control even if the control reproduction number is less than unity. We simulated the optimal control system with respect to denial and without denial. The numerical examples show that strategies with inhibition factors (without denial effect) are capable of reducing corona virus in the population. However, introducing denial into the system destabilizes it and renders the controls ineffective. Again, the results obtain from the comparison of the optimal control with constant control systems shows that timely implementation of these strategies is key in controlling the rapid spread of Corona virus disease. In Africa, COVID-19 is erroneously assumed to be a disease of White men and rich men who travel abroad. Thus most people in urban slums and rural areas refuse to adhere to control measures such as social distancing, wearing face masks, hand washing with water and soups, hand sanitizers e.t.c. This poses a challenge to the control of COVID-19 in Africa. It is therefore advocate that governments at all levels should carry out public health education to dispel this erroneous behaviour of their citizens that drive the spread of COVID-19. Eradicating the denial of the existence of COVID-19 is the first line of control before any form of interventions that will help to limit the spread of the disease.

Funding

This research did not receive any specific grant from funding agencies, commercial, or not-for-profit sectors.

Declaration of Competing Interest

The authors declare that they have no known competing financial interests or personal relationships that could have appeared to influence the work reported in this paper.

Supplementary material

Supplementary material associated with this article can be found, in the online version, at 10.1016/j.sciaf.2021.e00811

References

[1] L. Alanagreh, F. Alzoughool, M. Atoum, The human corona virus disease COVID-19: its origin, characteristics, and insights into potential drugs and its mechanisms, Pathogens 9 (5) (2020) 331, doi:10.3390/pathogens9050331.
[2] H.P. Singh, V. Khullar, M. Sharma, Estimating the impact of COVID-19 outbreak on high risk age group population in india, Augmented Human Research 5 (1) (2020) 18, doi:10.1007/541133-020-00037-9.
[3] K. Liang, Mathematical model of infection kinetics and its analysis for COVID-19, SARS and MERS, Infection, Genetics and Evolution 82 (2020) 104306, doi:10.1016/j.meegid.2020.104306.
[4] WHO(a), Coronavirus disease 2019 (COVID-19) situation report-51. accessed from https://reliefweb.int⟩report⟩china on March 11, 2020 (2020).
[5] WHO(b), Coronavirus disease 2019 (COVID-19) situation report-94, accessed ON july from https://www.who.int⟩coronavirus, on July 29, 2020 (2020).
[6] WHO, EMRO, Questions and answers COVID-19 health topics. accessed from https://www.emro.who.int⟩corona-virus, 2020(2020).
[7] ECDC, Covid-19 situation update world wide. retrieved from https://www.ecdc.europa.eu⟩giographic-distribution-world-wide on January, 2021 (2021).
[8] NCDC, Covid-19 situation report-182. retrieved from www.covid19.ncdc.gov.ng on august 30, 2020 (2021).
[9] P. Tmes, Shock as nigerian professor says COVID-19 does not exist. retrieved from www.premiumtimesng.com on July 7, 2020(2020).
[10] S.C. Kalichman, L. Eaton, C. Cherry, There is no proof that HIV causes AIDS. AIDS denialism beliefs among people living with HIV/AIDS, J Behav Med 33 (6) (2010) 432–440.
[11] S.T.C. Smith, S.P. Novella, HIV Denial in the internet era, J Behav Med 4 (8) (2007) e256, doi:10.1371/journal.pmed.0040256.
[12] J. Gachohi, S. Karanja, C. Mwangi, Challenges facing harm reduction interventions in the era of COVID-19 in africa, Scientific African 9 (2020) e00506.
[13] B. Dubey, A. Patra, P.K. Srivastava, U.S. Dubey, Modelling and analysis of an SEIR model with different types of nonlinear treatment rates, Journal of Biological Systems 21 (3) (2013) 1350023, doi:10.1142/5021833901350023X.

[14] R.K. Naji, B.H. Abdulateef, The dynamics of SLIR model with nonlinear incidence rate and saturated treatment function, Sci. Int. (Lahole) 29 (6) (2017) 1223–1236.
[15] R.K. Upandhyay, A.K. Pal, S. Kumari, P. Roy, Dynamics of an SEIR epidemics model with nonlinear incidence and treatment rates, Nonlinear Dyn 96 (2019) 2351–2368.
[16] J.N. Ndam, Modelling the impacts of lockdown and isolation on the eradication of COVI-19, BIOMATH 9 (2) (2020) 2009107, doi:10.11145/j.biomath.2020.09.107.
[17] D.A. Oluyori, H.O. Adebayo, Global analysis of an SEIRS model for covid-19 capturing saturated incidence with treatment response, MedRxiv preprint, (2020), doi:10.1101/2020.05.15.20103630. 2020
[18] D.O. Daniel, Mathematical model for the transmission of COVID-19 with non-linear forces of infection and the need for prevention measures in nigeria, Journal of Infectious disease and epidemiology 6 (5) (2020) 1–12, doi:10.23937/2474-3658/1510158.
[19] A.M. ELaiw, S.A. Azoz, Global proportion of a class HIV infection modelling with beddington-de angelis functional response, Mathematical Methods in the Applied Science 36 (2013) 383–394.
[20] A. Kaddar, Stability analysis in a delayed SIR epidemic with saturated incidence rate, Nonlinear Analysis Modelling and Control 15 (3) (2010) 299–309.
[21] G. Huang, W.M.n.Y. Takeuchi, Global analysis for delay virus dynamics model with beddington - de angelis functional response, Appl Math Lett 24 (2011) 1199–1203.
[22] B. Dubey, P. Dubey, U.S. Dubey, Dynamics of an SIR model with nonlinear incidence and treatment rate, Applications and Applied Mathematics: An International Journal 10 (2) (2016) 718–737.
[23] Y. Xing, Z. Guo, J. Liu, Backward bifurcation in a malaria transmission model, J Biol Dyn 14 (1) (2020) 368–388.
[24] M.O. Adeniyi, M.I. Ekum, C. Iluno, A.S. Ogunsanya, J.A. Akinyemi, S.I. Oke, M.B. Matadi, Dynamic model of COVID-19 disease with exploratory data analysis, Scientific African 000 (2020) e00477, doi:10.1016/j.sciaf.2020.e00477.
[25] M.K. Adeyeri, S.P. Ayodeji, A.O. Orisawayi, Development of a dual-purpose wheelchair for COVID-19 paraplegic patients using nigerian anthropometry data, Scientific African 9 (2020) e00547.
[26] A.M.S. Sayedahmed, A.A.A. Abdalla, M.H.M. Khalid, Knowledge, attitude and practice regarding COVID-19 among sudanese population during the early days of the pandemic: online cross-sectional survey, Scientific African 10 (2020) e00652.
[27] F.S. Alshammari, A mathematical model to investigate the transmission of COVID-19 in the kingdom of saudi arabian, Comput Math Methods Med 9136157 (2020) 1–13.
[28] C.T. Deressa, G.F. Duressa, Modelling and optimal analysis of transmission dynamics of COVID-19: the case of ethiopia, Alexandria Engineering Journal 60 (2021) 719–732.
[29] A.B. Gumel, E. Iboi, O.O. Sharomi, C. Ngonghala, Mathematical modelling and analysis of COVID-19 pandemic in nigeria, MedRxiv preprint (2020), doi:10.1101/2020.05.22-20110387.
[30] L. Perko, Differential Equations and Dynamical systems, Springer Science and Business Media, 2013.
[31] P.V.d. Driessche, J. Watmough, Reproduction numbers and sub-threshold endemic equilibria for compartmental models of disease transmission, Journal of Mathematical Biosciences 180 (2002) 29–48.
[32] M. Martcheva, An Introduction to Mathematical Epidemiology, volume 61, Springer Science and Business Media, 2015.
[33] A.B. Gumel, O. Sharomi, Re-infection-induced backward bifurcation in the transmission dynamics of chlamydia trachomatis, J Math Anal Appl 356 (2009) 96–118.
[34] C. Castillo-Chavez, B. Song, Dynamical models of tuberculosis and their applications, Mathematical Biosciences and Engineering 1 (2) (2004) 361–404.
[35] J.P. La Salle, The Stability of Dynamical Systems, Hamilton Press, Berlin, New Jersey, USA, 1976.
[36] S. Olaniyi, O.S. Obabiyi, Qualitative analysis of malaria dynamics with nonlinear incidence functions, Applied Mathematical Sciences 8 (78) (2014) 3889–3904.
[37] H.T. Fatmawati, U.D. Purwati, F. Riyudha, H. Tasman, Optimal control of discrete age-structured model for tuberculosis transmission, Heliyon 6 (2020) e03030.
[38] C.E. Madubueze, S. Dachollom, I.O. Onwubuya, Controlling the spread of COVID-19 control analysis, Comput Math Methods Med 6862516 (2020) 1–14.